2003

Methyl and T-Butyl Group Reorientation in Planar Aromatic Solids: Low-Frequency Nuclear Magnetic Resonance Relaxometry and X-Ray Diffraction

Peter A. Beckmann
Bryn Mawr College, pbeckman@brynmawr.edu

Carylon Buser

Kathleen Gullifer

Frank B. Mallory
Bryn Mawr College, fmallory@brynmawr.edu

Clelia W. Mallory

See next page for additional authors

Custom Citation

P.A. Beckmann, C.A. Buser, K. Gullifer, F.B. Mallory, C.W. Mallory, G.M. Rossi, A.L. Rheingold. *J. Chem. Phys.* **118** (24), 11129 (2003).

Authors
Peter A. Beckmann, Carylon Buser, Kathleen Gullifer, Frank B. Mallory, Clelia W. Mallory, Gene M. Rossi, and Arnold L. Rheingold

Methyl and *t*-butyl group reorientation in planar aromatic solids: Low-frequency nuclear magnetic resonance relaxometry and x-ray diffraction

Peter A. Beckmann[a)]
Department of Physics, Bryn Mawr College, Bryn Mawr, Pennsylvania 19010-2899 and Department of Chemistry and Biochemistry, University of Delaware, Newark, Delaware 19716-2522

Carolyn A. Buser[b)]
Department of Physics and Department of Chemistry, Bryn Mawr College, Bryn Mawr, Pennsylvania 19010-2899

Kathleen Gullifer[c)]
Department of Physics, Bryn Mawr College, Bryn Mawr, Pennsylvania 19010-2899

Frank B. Mallory
Department of Chemistry, Bryn Mawr College, Bryn Mawr, Pennsylvania 19010-2899

Clelia W. Mallory
Department of Chemistry, University of Pennsylvania, Philadelphia, Pennsylvania 19104-6323

Gene M. Rossi and Arnold L. Rheingold[d)]
Department of Chemistry and Biochemistry, University of Delaware, Newark, Delaware 19716-2522

(Received 4 March 2002; accepted 17 March 2003)

We have synthesized 3-*t*-butylchrysene and measured the Larmor frequency $\omega/2\pi$ (= 8.50, 22.5, and 53.0 MHz) and temperature T (110–310 K) dependence of the proton spin–lattice relaxation rate R in the polycrystalline solid [low-frequency solid state nuclear magnetic resonance (NMR) relaxometry]. We have also determined the molecular and crystal structure in a single crystal of 3-*t*-butylchrysene using x-ray diffraction, which indicates the presence of a unique *t*-butyl group environment. The spin-1/2 protons relax as a result of the spin–spin dipolar interactions being modulated by the superimposed reorientation of the *t*-butyl groups and their constituent methyl groups. The reorientation is successfully modeled by the simplest motion; that of random hopping describable by Poisson statistics. The x-ray data indicate near mirror-plane symmetry that places one methyl group nearly in the aromatic plane and the other two almost equally above and below the plane. The NMR relaxometry data indicate that the nearly in-plane methyl group and the entire *t*-butyl group reorient with a barrier of 24.2 ± 0.9 kJ mol^{-1}, and the two out-of-plane methyl groups reorient with a barrier of 14.2 ± 0.6 kJ mol^{-1}. Following a brief review of methyl group rotation in simple ethyl-, and isopropyl-substituted one- and two-ring aromatic van der Waals molecular solids, the barriers for the out-of-plane methyl groups and the *t*-butyl group in 3-*t*-butylchrysene are compared with those barriers in three related molecular solids whose crystal structure is known: 4-methyl-2,6-di-*t*-butylphenol, 1,4-di-*t*-butylbenzene, and polymorph *A* of 2,6-di-*t*-butylnaphthalene. A trend is observed in the reorientational barriers for the *t*-butyl and the out-of-plane methyl groups across this series of four compounds: as the *t*-butyl barriers decrease, the out-of-plane methyl barriers increase. © *2003 American Institute of Physics.* [DOI: 10.1063/1.1575202]

I. INTRODUCTION

Low-frequency nuclear magnetic resonance (NMR) relaxometry and single-crystal x-ray-diffraction probe very different time scales and the two techniques can be combined to investigate structure and dynamics in ways that neither can do alone. A class of molecules that has been rewarding to study are single- and fused-ring aromatic structures containing one or two *t*-butyl groups.[1–8] We have synthesized the organic molecule 3-*t*-butylchrysene, determined the molecular (Fig. 1) and crystal (Figs. 2 and 3) structures, and measured the proton spin–lattice relaxation rate R as a function of temperature T and Larmor frequency $\omega/2\pi$ (Fig. 4). We have chosen to report our work on 3-*t*-butylchrysene because of its unusual R versus T behavior. Of the many systems

a)Electronic mail: pbeckman@brynmawr.edu
b)Current address: Merck, Cancer Research Department, WP16-315, Sumneytown Pike, West Point, PA 19486.
c)Current address: Defense Supply Center Philadelphia, 700 Robbins Avenue, Philadelphia, PA 19111.
d)Current address: Department of Chemistry and Biochemistry, University of California, San Diego, La Jolla, CA 92093.

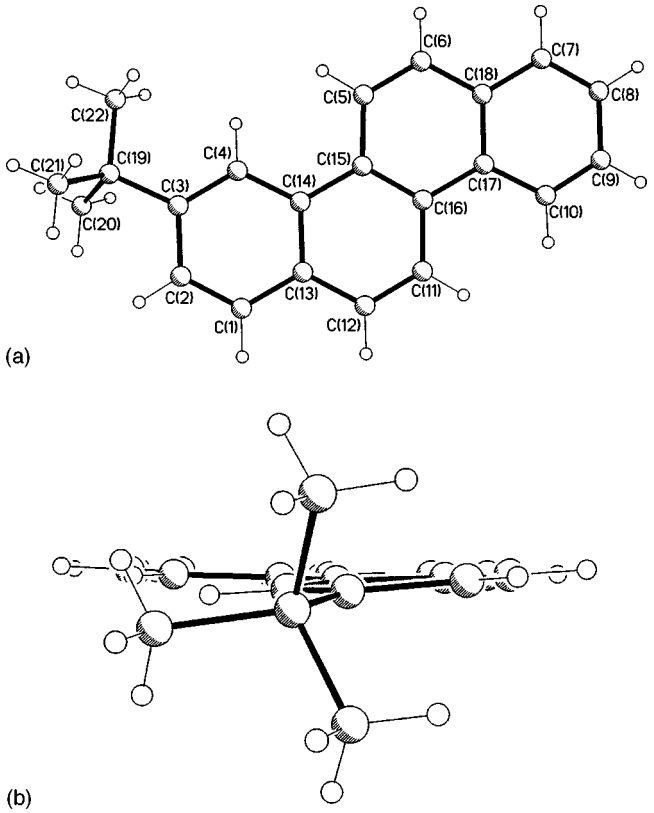

FIG. 1. Molecular structure of 3-*t*-butylchrysene. (a) The four-ring structure with the *t*-butyl group in the 3-position. (b) An end view in the plane of the ring structure. In the crystal, all *t*-butyl groups are equivalent.

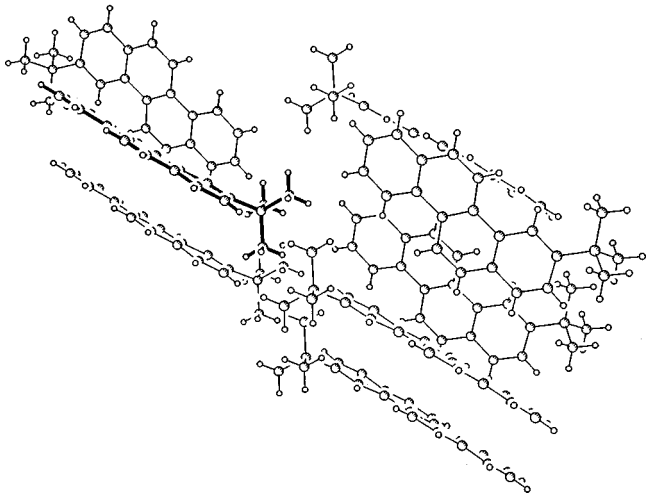

FIG. 3. A picture of the crystal structure of crystalline 3-*t*-butylchrysene showing the interaction among *t*-butyl groups on different molecules. One molecule is highlighted for clarity.

studied to date, it serves as a ''missing link'' and has resulted in our suggesting a new model for *t*-butyl group reorientation.

X-ray diffraction probes electron densities over time scales characteristic of the photon–electron interaction (10^{-19} s) and as such sees time averages of essentially instantaneous structures on the time scale for any molecular motions. Average structures (atomic positions) can then be determined from the electron density configurations using sophisticated algorithms.[9] The structures so determined can then be correlated with low-frequency NMR relaxometry results which are sensitive to the reorientation of the *t*-butyl groups and their constituent methyl groups. It is important that the proton NMR relaxometry be performed at *low* frequencies in order to match the NMR frequency with the frequencies of the motions of interest. Thus the ideal conditions for proton NMR *relaxometry* are in marked contrast to proton NMR *spectroscopy* where the current drive is to higher frequencies (in order to better resolve chemical shifts).

Proton NMR relaxometry and x-ray diffraction are both very old techniques and they have been used together for many years on a variety of systems. However, there are important unanswered questions concerning the relationship between structure and motion in a large variety of solids and the research remains fruitful. The two techniques have been combined to better understand dynamics in ionic solids.[10–14] In these cases, motions involve ion reorientation and translation. The two techniques have come together to better understand methyl group reorientation in 4,5-dimethylphenanthrene where the crowded conditions distort the otherwise planar aromatic ring[15,16] and to study the complex motions in 1-bromo and 1-iodo-adamantane.[17] Recently, the two techniques together have allowed the development of a model for methyl group reorientation in tetrapentylammonium iodide.[18]

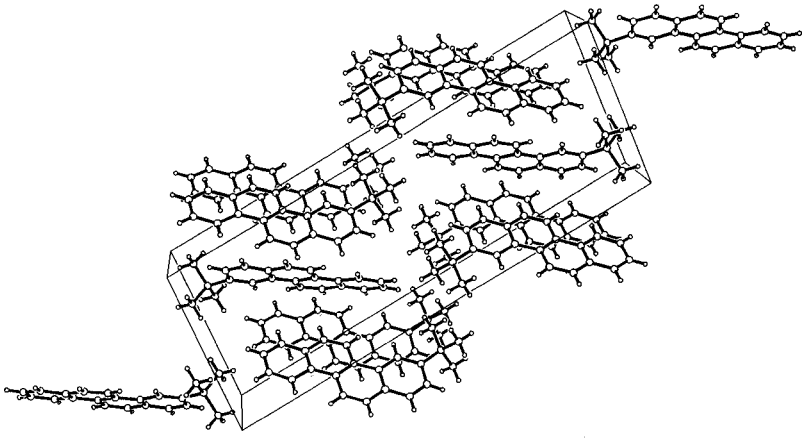

FIG. 2. The unit cell of 3-*t*-butylchrysene. There are four molecules per unit cell with the figure showing more than the two whole and four half molecules in the unit cell.

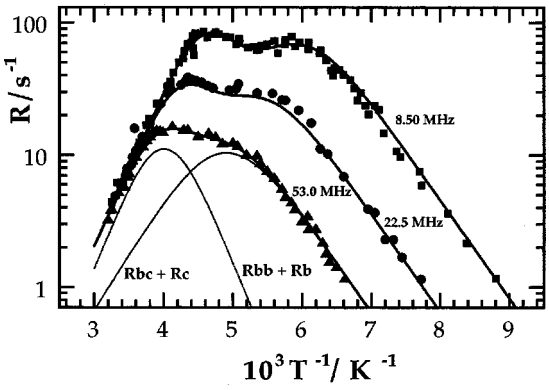

FIG. 4. Proton Zeeman relaxation rate R (on a logarithmic scale) vs inverse temperature T^{-1} in polycrystalline 3-*t*-butylchrysene, at three Larmor frequencies as indicated. The *single* five-parameter fit shown at *all three* frequencies is discussed in the text. The contributions to R from the two inequivalent types of rotors are indicated for 53.0 MHz. The R maximum at $T=250$ K ($10^3T^{-1}=4$ K^{-1}) at 53.0 MHz and shifting to lower temperatures at lower Larmor frequencies results from the reorientation of *both* the *t*-butyl group *and* the reorientation of the (nearly) in-plane methyl group superimposed on the reorientation of the *t*-butyl group. This is $R_{bb}+R_b$ in Eq. (11). The R maximum at $T=200$ K ($10^3T^{-1}=5$ K^{-1}) at 53.0 MHz and shifting to lower temperatures at lower Larmor frequencies results from the reorientation of the two out-of-plane methyl groups in the *t*-butyl group [Fig. 1(b)] superimposed on the slower reorientation of the entire *t*-butyl group. This is $R_{bc}+R_c$ in Eq. (11). Note that the two motions are more clearly resolved at the lowest NMR frequency.

These systems tend to be more complicated, either structurally or dynamically or both, than the systems we are studying.

Deuteron NMR has also been used very successfully in conjunction with x-ray diffraction. Deuteron NMR has the advantage (over proton NMR) that the spectra of the former can reveal motional information[19,20] whereas proton spectra are broad (tens of kHz) and featureless due to strong spin–spin couplings. Deuteron relaxation rates are dominated by local interactions (the electric field gradient in the D–X bond).[19,21,22] This is a simplifying factor and can be an advantage in modeling the motion so long as the quadrupolar coupling constant (related to the width of the spectrum) can itself be adequately modeled. Proton relaxation rate studies, on the other hand, have the advantage that the hydrogen atoms under study can interact strongly with nearby hydrogen atoms (spin–spin interactions) and this gives a window on relating the observed relaxation rates to both the local and the longer-range structures of the solid. Deuteron NMR spectroscopy and relaxation rate studies[23] and x-ray diffraction[24] have been combined to show that there are two chemically inequivalent methyl group sites in alpha-crystallized toluene. A truly beautiful, more recent deuteron spectroscopy and relaxation rate study in 2,3-dimethylnaphthalene[25] exploited the known crystal structure[26] to relate the disordered structure of this solid with models for methyl group reorientation. Finally, deuteron NMR spectroscopy, deuteron NMR relaxation rate studies, and x-ray diffraction have teamed up to better model the relationship between the complicated motions and aromatic ring distortions in 9-*t*-butylanthracene[27] as well as the dynamical behavior of *t*-butyl reorientation in 1,4-di-*t*-butylbenzene in inclusion compounds.[2]

The main purposes of this paper are (1) to present the synthesis, the x-ray diffraction, and the temperature and frequency dependence of the proton spin–lattice relaxation rate in solid 3-*t*-butylchrysene, (2) to review the current dynamical model for *t*-butyl and methyl group motion and recast it in a more general way, and (3) to compare proton NMR relaxometry and x-ray diffraction studies of three other molecular solids with the results in 3-*t*-butylchrysene presented here. The three other systems are 4-methyl-2,6-di-*t*-butylphenol, 1,4-di-t-butylbenzene, and polymorph *A* of 2,6-di-*t*-butylnaphthalene. These four van der Waals solids have the important property that the molecular structure in the crystal is not expected to be appreciably different from the isolated molecule structure, except, perhaps, for the orientation of the *t*-butyl groups. This results in an approach which considers the solid, to first approximation, as simply holding the molecules fixed, meaning that the aromatic backbone does not engage in motions on the NMR time scale. The dynamics of the *t*-butyl group, then, can be considered in terms of the isolated molecule with the neighboring molecules treated as a perturbation. We find that the results for 3-*t*-butylchrysene do not fit our far-too-neat previously developed model and we outline, qualitatively, a new model for methyl and *t*-butyl group reorientation that needs to be further developed quantitatively.

II. EXPERIMENT

A. Sample preparation

3-*t*-Butylchrysene was synthesized from commercially available materials by a two-step process: a Wittig reaction of 1-naphthaldehyde with the phosphonium salt obtained from the treatment of 4-*t*-butylbenzyl bromide with triphenylphosphine, followed by photocyclization[28] of the resulting diarylethylene derivative.

1. (E)-1-(4′-t-Butylstyryl)naphthalene

A Wittig reaction of 1-naphthaldehyde with the ylid derived from (4-*t*-butylbenzyl)triphenylphosphonium bromide gave a mixture of the *E* and *Z* isomers of 1-(4′-*t*-butylstyryl)naphthalene. This mixture was isomerized in cyclohexane solution by catalysis by atomic iodine (produced from I_2 by irradiation with visible light) to give the pure *E* isomer (76%). Recrystallization from methanol gave material with mp 91.4–92.0 °C. ^{1}H NMR ($CDCl_3$, 300 MHz) δ 8.22 (*br d*, $J=8$ Hz, 1 H; H-8), 7.86 (*br d*, $J=8$ Hz, 1 H; H-5), 7.85 (*d*, $J=16.0$ Hz, 1 H; H-α), 7.79 (*br d*, $J=8.2$ Hz, 1 H; H-4), 7.74 (*br d*, $J=7.2$ Hz, 1 H; H-2), 7.55 (*d*, $J=8.4$ Hz, 2 H; H-2′ and H-6′), 7.52–7.47 (m, 2 H; H-6 and H-7), 7.48 (*br t*, $J=7.7$ Hz, 1 H; H-3), 7.43 (*d*, $J=8.4$ Hz, 2 H; H-3′ and H-5′), 7.14 (*d*, $J=16.0$ Hz, 1 H; H-α′), 1.36 (s, 9 H; $(CH_3)_3C$). Anal.[29] Calcd. for $C_{22}H_{22}$: C, 92.31; H, 7.69. Found: C, 92.25; H, 7.49.

2. 3-t-Butylchrysene

A magnetically stirred solution of 2.84 g (10 mmol) of (*E*)-1-(4′-*t*-butylstyryl)naphthalene and 0.254 g (1 mmol) of I_2 in 1.1 L of cyclohexane was irradiated for 3.5 h with

ultraviolet light from a 450 W Hanovia mercury lamp. When the reaction was judged to be substantially complete by GC/MS analysis, the solvent was removed by rotary evaporation and the residue was chromatographed on alumina using hexanes as eluent. Evaporation of the solvents and recrystallization of the resulting solid from hexanes gave 1.4 g (50%) of 3-*t*-butylchrysene, mp 114.0–114.7 °C. Further purification by an additional recrystallization from hexanes gave material with mp 117.2–117.8 °C. ^{1}H NMR ($CDCl_3$, 300 MHz) δ 8.77 (*br d*, J=8.2 Hz, 1 H; H-10), 8.75 (*br s*, 1 H; H-4), 8.74 (*d*, J=8.9 Hz, 1 H; H-5), 8.66 (*d*, J=9.0 Hz, 1 H; H-11[30]), 8.00 (*d*, J=8.9 Hz, 1 H; H-6[30]), 7.99 (*dd*, J=7.8 Hz and 1.4 Hz, 1 H; H-7), 7.96 (*d*, J=9.2 Hz, 1 H; H-12[30]), 7.93 (*d*, J=8.3 Hz, 1 H; H-1), 7.72 (*dd*, J=8.4 Hz and 1.9 Hz, 1 H; H-2), 7.69 (*ddd*, J=8.2 Hz, 6.8 Hz, and 1.6 Hz, 1 H; H-9), 7.62 (*ddd*, J=7.9 Hz, 6.9 Hz, and 1.1 Hz, 1 H; H-8), 1.53 (*s*, 9 H; $(CH_3)_3C$). Anal.[29] Calcd. for $C_{22}H_{20}$: C, 92.96; H, 7.04. Found: C, 93.16; H, 6.87.

B. X-ray diffraction

3-*t*-Butylchrysene crystallizes as exceedingly thin plates. A specimen was successfully mounted by suspending it in a film of a glycerine emulsion cooled to 173 K. Reflections making a glancing angle of less than 3° to the major face [0,0,1] were excluded. Nonetheless, a combination of edge distortions, high anisotropy in the reflection data, and inevitable curvature of the crystal from mounting stresses produced a data collection of limited quality. The data reported were the best of three sets. The crystal was found to belong to the monoclinic crystal system and systematic absences in the diffraction data uniquely assigned the space group as $P2_1/n$ [a=9.7202(12), b=6.1898(7), c=26.791(3) Å, β=97.011(2)°, V=1599.9(3) Å^3, Z=4]. Using a Siemens P4 four-circle diffractometer equipped with a SMART CCD detector and MoKα radiation (λ=0.71073 Å), 1225 frames were collected in 0.3° increments with 30 s exposures. Of 4798 reflections harvested from these frames, 2068 were unique. The structure was solved by direct methods and completed by a series of difference Fourier syntheses. All nonhydrogen atoms were refined anisotropically and all hydrogen atoms were incorporated as idealized contributions. At convergence: $R(F)$=0.099, $R(wF^2)$=0.252. All software is contained in the libraries maintained by Bruker AXS, Madison, WI, and include SHELXTL 5.1, SMART, and SAINT. A CIF file containing detailed crystallographic information may be obtained from one of the authors (A.L.R.) or from the Cambridge Structural Database where the data have been deposited. The molecular structure is shown in Fig. 1, the unit cell is shown in Fig. 2, and the environments of a set of *t*-butyl groups are shown in Fig. 3.

C. NMR relaxometry

The temperature T dependence of the proton spin–lattice relaxation rate R was measured using standard inversion-recovery pulse NMR techniques[21] at temperatures T between 110 and 310 K at Larmor frequencies of $\omega/2\pi$=8.50, 22.5, and 53.0 MHz, corresponding to magnetic fields $B=\omega/\gamma$ of 0.200, 0.528, and 1.24 T [for proton gyromagnetic ratio γ with $\gamma/(2\pi)$=42.577 MHz/T]. Three fixed-frequency CPS-2 Spin-Lock pulsed NMR spectrometers were used with variable-field electromagnets. The nonexponential free induction decay following the amplifier recovery was reasonably well-characterized by a relaxation time of about 20 μs, corresponding to a spin–spin relaxation rate R_2 of about 5×10^4 s^{-1}. This is 600 times greater than the largest spin–lattice rate R measured and indicates rapid spin diffusion.

Temperature was varied by means of a flow of cold nitrogen gas which was recooled and reheated at various stages in order to vary and regulate the temperature. The variable temperature system was home-made. The polycrystalline sample was placed in a 7-mm-i.d. tube containing a 20 mm length of sample, 15 mm of which was within the NMR coil. Temperature was determined with a calibrated copper–constantan thermocouple, which was buried inside the sample 2 mm outside the NMR coil. Between measurements, 30–45 min was allowed to elapse to ensure equilibrium after a temperature change. Absolute temperature was determined to within $\pm$2 K and temperature differences could be monitored to within $\pm$30 mK. Temperature gradients along the sample could be determined by changing the position of the thermocouple. At $\pm$0.5 K at the lowest temperature (and progressively less at higher temperatures), from one end of the sample to the other (within the NMR coil), these gradients are negligible compared with the temperature dependence of the measured R values.

The data are presented as $\ln R$ versus T^{-1} in Fig. 4. The uncertainties on the R measurements ranged from $\pm$2% to $\pm$8%, and the sizes of the symbols in Figure 4 are chosen to reflect $\pm$5% error flags. The scatter in the data is consistent with the uncertainties associated with each individual measurement.

III. SPIN RELAXATION THEORY AND APPLICATIONS TO *t*-BUTYL GROUPS: A BRIEF REVIEW

The observed proton spin–lattice relaxation rate is written[5]

$$R=\sum_{i=1}^{M}\left[\frac{9}{N}R_i^{\text{inter}}+\sum_{j=1}^{3}\frac{3}{N}R_{ij}^{\text{intra}}\right], \tag{1}$$

where R_{ij}^{intra} is the relaxation rate due to the modulation of the dipole–dipole interactions between the three protons (spins) in the jth methyl group, which, in turn, resides in the ith *t*-butyl group. The index j runs over the three methyl groups in the ith *t*-butyl group. R_i^{inter} is the relaxation rate due to the modulation of the dipole–dipole interactions between the inter-methyl, intra-*t*-butyl protons for the ith *t*-butyl group. There are M crystallographically distinct *t*-butyl groups. M=1 for 3-*t*-butylchrysene.

As outlined in the following, R_{ij}^{intra} takes into account the interactions among the three protons in each methyl group exactly (within the confines of the model). The ratio *3/N* is the ratio of the number of protons in a methyl group to the number of protons in the chemically distinct unit, in the case of 3-*t*-butylchrysene, a single molecule. Thus, N=20 for 3-*t*-

butylchrysene. This assumes that spin diffusion is rapid and that the nuclear magnetization is always equally spread among all protons in the molecule. Experimentally, this is indicated by the fact that the spin–spin relaxation rate R_2 is very much greater than the spin–lattice relaxation rate R.

In the following, R_i^{inter} is determined by an approximation and the factor $9/N$ in Eq. (1) is the ratio of the number of protons in a *t*-butyl group to the number of protons in the chemically distinct unit. Although the assumptions leading to Eq. (1) (exponential relaxation, additivity of rates, etc.) are reasonable for liquids, careful justification is required for using this model to describe the spin–lattice relaxation resulting from methyl and *t*-butyl group reorientation in polycrystalline solids. These assumptions and their rationale are carefully laid out elsewhere.[22,31]

If the reorientation of the *j*th methyl group in the *i*th *t*-butyl group is characterized by the correlation time τ_{ij} and the reorientation of the *i*th *t*-butyl group is characterized by the correlation time τ_i, R_{ij}^{intra} is given by[5,7,8]

$$R_{ij}^{\text{intra}}=\tfrac{4}{3}A^{\text{intra}}\left[\tfrac{2}{9}h(\omega,\tau_{ij})+\tfrac{2}{9}h(\omega,\tau_i)+\tfrac{19}{36}h(\omega,\tau_{i,ij})\right], \tag{2}$$

with

$$h(\omega,\tau)=j(\omega,\tau)+4j(2\omega,\tau), \tag{3}$$

for reduced spectral density $j(\omega,\tau)$. The first and second terms of Eq. (2) correspond to methyl group and *t*-butyl group reorientation, respectively, and the third term, with $\tau_{i,ij}^{-1}=\tau_i^{-1}+\tau_{ij}^{-1}$ corresponds to the superposition of the two motions.

The reduced spectral density for the simplest dynamical model for methyl group and *t*-butyl group reorientation comes from thermally assisted random (Poisson) hopping,[21,22]

$$j(\omega,\tau)=\frac{2\tau}{(1+\omega^2\tau^2)}. \tag{4}$$

Independently, we assume τ can be modeled by an Arrhenius relationship;

$$\tau=\tau_\infty\exp\left(\frac{E}{kT}\right). \tag{5}$$

For a barrier $E\gg kT$ (for example, 12 kJ mol^{-1} $=1.5\times10^3$ K), the methyl group spends most of its time at the bottom of the barrier and in a very simple, but nonetheless, appealing model, τ_∞^{-1} can be identified with the attempt frequency $\tilde{\tau}_\infty^{-1}$ for crossing the barrier (i.e., methyl group rotates by $2\pi/3$). In the harmonic approximation, $\tilde{\tau}_\infty^{-1}$ is given by[32]

$$\tilde{\tau}_\infty=\frac{2\pi}{3}\left(\frac{2I}{E}\right)^{1/2}, \tag{6}$$

where I is the moment of inertia of the group. Once E and τ_∞ have been determined by fitting data, it is convenient to express the fitted τ_∞ in units of $\tilde{\tau}_\infty$. It's just a convenient, classical, benchmark.

The dipole–dipole strength parameter in Eq. (2) is

$$A^{\text{intra}}=\frac{9}{40}\left(\frac{\mu_0}{4\pi}\right)^2\left(\frac{\hbar\gamma^2}{r^3}\right)^2=3.80\times10^9\ \text{s}^{-2}, \tag{7}$$

for proton magnetogyric ratio $\gamma=2.675\times10^8$ kg^{-1} s A, $\mu_0/4\pi=10^{-7}$ m kg s^{-2} A^{-2} where μ_0 is the permeability of free space (now often referred to as the magnetic constant), and proton–proton separation $r=1.79\times10^{-10}$ m in a methyl group. This value of r assumes an idealized tetrahedral geometry with idealized C–H bond lengths. The factor 9/40 can be conveniently, although somewhat artificially, factored into the products 2(3/4)(3/20). The factor $[(3/20)\ (\mu_0/4\pi)^2(\gamma^4\hbar^2/r^6)]$ is a convenient starting point and comes from the basic relaxation theory for a pair of spin-1/2 particles undergoing isotropic reorientation [Ref. 22, p. 300, Eq. (105) (with $(\mu_0/4\pi)^2$ inserted to give SI units)]. The factor 3/4 can be thought of as a correction for the fact that the motion of any given ^{1}H–^{1}H vector is not isotropic but confined to a plane. The factor 2 comes from the fact that each ^{1}H spin in the methyl group is involved in two spin–spin interactions. We note that this definition of A^{intra} differs from that in Ref. 5 by the factor 9/40.

To compute R_i^{inter} in Eq. (1), we first note that if $\tau_i=\infty$ (no *t*-butyl group reorientation), then $\tau_{i,ij}=\tau_{ij}$ and Eq. (2) reduces to $R_{ij}^{\text{intra}}=A^{\text{intra}}\,h(\omega,\tau_{ij})$. We condense each of the three protons in a methyl group to the center of their reorientation axis and consider a *t*-butyl group to be an ensemble of three such moieties. R_i^{inter}, the relaxation rate due to the reorientation of this ensemble, will be

$$R_i^{\text{inter}}=3A^{\text{inter}}h(\omega,\tau_i), \tag{8}$$

with

$$A^{\text{inter}}=\frac{9}{40}\left(\frac{\mu_0}{4\pi}\right)^2\left(\frac{\hbar\gamma^2}{r_*^3}\right)^2 \tag{9}$$

$$=\left(\frac{r}{r_*}\right)^6A^{\text{intra}}=1.40\times10^8\text{s}^{-2}, \tag{10}$$

where $r_*=3.12\times10^{-10}$ m assumes an idealized tetrahedral geometry with idealized bond lengths. The x-ray data accurately position the four carbon atoms in the *t*-butyl group and show the departure from this idealized geometry is very minor and, within the framework of the approximation being used here, the differences between the idealized and observed C–C–C bond angles and CC lengths are negligible. The factor 3 in Eq. (8) accounts for the fact that each ''spin'' in the rotor is a trio of spins. We note that this definition of A^{inter} differs from that in Ref. 5 by the factor 9/40.

The relaxation rate data in Fig. 4 show that there are two distinct correlation times τ. Indeed, at $\omega/2\pi=8.50$ MHz, the two maxima in R due to the conditions $\omega\tau\approx1$ for each τ are clearly resolved. The x-ray data show that in 3-*t*-butylchrysene there is one chemically and crystallographically distinct *t*-butyl group per unit cell. In this case, there is one term in the sum over i in Eq. (1) (i.e., $M=1$) and $N=20$

is the number of protons in the molecule. Further, as shown in Fig. 1, the x-ray data show that one methyl group lies nearly in the plane of the adjacent aromatic ring and that the other two methyl groups lie above and below this plane, respectively. We have analyzed the data using the two possible ways that give rise to two correlation times (with the boundary condition that all *t*-butyl groups are equivalent). In one model, the three methyl groups reorient at one rate and the *t*-butyl group reorients at another rate. In the other model, two methyl groups reorient at one rate and both the third methyl group (presumably the one nearly in the plane) and the *t*-butyl group reorient at the other rate. The former model does not work and we present the details for the latter, noting that modeling the former from the details of the latter is not difficult.

Referring to the sums over i and j in Eq. (1), the reorientation of the two out-of-plane groups is characterized by $\tau_{11}=\tau_{12}=\tau_c$ and, the reorientation of the (nearly) in-plane methyl group and the entire *t*-butyl group are characterized by $\tau_{13}=\tau_1=\tau_b$. With $\tau_{bc}^{-1}=\tau_b^{-1}+\tau_c^{-1}$ and $\tau_{bb}^{-1}=\tau_b^{-1}+\tau_b^{-1}=2\tau_b^{-1}$ and Eqs. (2) and (8) substituted into Eq. (1) yield

$$R=R_b+R_{bb}+R_c+R_{bc} \tag{11}$$

$$=A_b\,h(\omega,\tau_b)+A_{bb}\,h(\omega,\tau_{bb})+A_c\,h(\omega,\tau_c)+A_{bc}\,h(\omega,\tau_{bc}), \tag{12}$$

with the theoretically determined values for the A given by

$$\tilde{A}_b=\frac{M}{N}\left[27A^{inter}+\frac{32}{9}A^{intra}\right]=\frac{M}{N}(1.73\times10^{10}\ \ s^{-2}), \tag{13}$$

$$\tilde{A}_{bb}=\frac{M}{N}\frac{19}{9}A^{intra}=\frac{M}{N}(8.03\times10^{9}\ \ s^{-2}), \tag{14}$$

$$\tilde{A}_c=\frac{M}{N}\frac{16}{9}A^{intra}=\frac{M}{N}(6.76\times10^{9}\ \ s^{-2}), \tag{15}$$

and,

$$\tilde{A}_{bc}=\frac{M}{N}\frac{38}{9}A^{intra}=\frac{M}{N}(1.61\times10^{10}\ \ s^{-2}), \tag{16}$$

for M chemically equivalent *t*-butyl groups and N protons in the molecule. We note that all four $\tilde{A}$ values are comparable, which is why very simplistic models that ignore these details are not helpful, even if they interpret the data fairly well. The term $27\,A^{inter}$ in Eq. (13) contributes 28% of $\tilde{A}_b$ while the term $(32/9)\,A^{intra}$ contributes 72%.

IV. DATA ANALYSIS

3-*t*-Butylchrysene crystallizes in a primitive monoclinic system without imposed crystallographic symmetry. The molecules form no close contacts at distances significantly less than the sum of their van der Waals radii. As shown in the unit-cell packing diagram (Fig. 2), molecules pack with their long axis aligned with the *c* crystal axis and alternate both in the orientation of the *t*-butyl groups and the plane of the aromatic system. This regime effectively prevents the formation of π-stacked interactions between aromatic planes. All *t*-butyl groups experience the same environment.

The temperature and Larmor frequency dependence of the spin–lattice relaxation rate $R(T,\omega)$ for polycrystalline 3-*t*-butylchrysene in Fig. 4 is fitted to the two-tau model discussed earlier. R is given by Eq. (12) with Eqs. (3), (4), and (5). The single set of three solid curves at the three Larmor frequencies $\omega/2\pi$ in Fig. 4 involve five adjustable parameters: E_b, E_c, $\tau_{b\infty}$, and $\tau_{c\infty}$ which come from Eq. (5) for the correlation times τ_b and τ_c and a common multiplicative factor $A/\tilde{A}$ for the four A values in Eq. (12), as discussed in the following paragraph. The partial sums R_b+R_{bb} and R_c+R_{bc} in Eq. (11) are shown at 53.0 MHz in Fig. 4. *Since all terms contribute significantly, it is necessary to account properly for the superimposed reorientation of the* t*-butyl group and their constituent methyl groups. Note that the two relaxometry peaks are better resolved at 8.50 MHz than they are at 53.0 MHz*.

The fitting parameter $A/\tilde{A}$ is defined by $A/\tilde{A}\equiv A_b/\tilde{A}_b=A_{bb}/\tilde{A}_{bb}=A_c/\tilde{A}_c=A_{bc}/\tilde{A}_{bc}$, where the numerical values of $\tilde{A}_b$, $\tilde{A}_{bb}$, $\tilde{A}_c$, and $\tilde{A}_{bc}$ are given by Eqs. (13)–(16). The effect, then, of this parameter is to move the entire relaxation curve up and down without changing its shape and without changing the relative contribution of the four contributions to the total R. The fitted value is $A/\tilde{A}=1.07\pm0.05$. The liberal uncertainty is arrived at by noting, visually, the effect of changing this parameter. This ratio would be unity if only intra *t*-butyl group spin–spin interactions were considered and if the approximation used for the inter-methyl, intra-*t*-butyl spin–spin interactions were perfect. The modulation of the latter interactions by *t*-butyl reorientation contributes about 28% to R_b or about 19% to R_b+R_{bb}, which together account for the maximum in R at 250 K ($10^3T^{-1}=4\ \ K^{-1}$) at 53.0 MHz as indicated in Fig. 4. If the approximation used for the inter-methyl, intra-*t*-butyl spin–spin interactions were in error by, say 25%, this would result in a change in $\tilde{A}_b$ by 7% and a change in the predicted value of R_b+R_{bb} and thus the fitted value of $A_b/\tilde{A}_b$ by about 5%.

More significantly, the theoretical values of the $\tilde{A}$ do not account for the spin–spin interactions between the nine *t*-butyl protons and all the other protons in the vicinity. The factor r^{-6} for proton–proton separation r ensures that these interactions will have a small effect because the three protons in a methyl group are so much closer to one another than they are to other protons in the molecule and to the protons in nearby molecules. Considering only the protons in the same molecule, an extension of the methods of Palmer[33]

suggests that the methyl proton–extra-*t*-butyl proton interactions would add terms to Eqs. (11) and (12) that would increase the fitted value of $A/\tilde{A}$ by about 5%–10% (from unity). Given all these matters, the fitted value of $A/\tilde{A}=1.07\pm0.05$ is very reasonable and consistent with the fitting model. *We note that a fitted value of $A/\tilde{A}$ significantly less than unity would be unacceptable and would require abandoning the model.*

The fitted activation energies are $E_b=24.2\pm0.9$ kJ mol^{-1} and $E_c=14.2\pm0.6$ kJ mol^{-1}, the uncertainties being about 4%. Fitting $\ln R$ versus T^{-1} regions at the highest and lowest temperatures to linear least-square fits gives an uncertainty of about 2% for each of these parameters. The other 2% comes from noting, visually, the effect of adjusting E_b and E_c on the total fit.

The fitted values of $\tau_{b\infty}$ and $\tau_{c\infty}$ are $\tau_{b\infty}=4.5\times10^{-13}$ s and $\tau_{c\infty}=2.0\times10^{-14}$ s with large uncertainties, about $\pm25\%$. Most of the uncertainty has its origin in the fact that when the activation energy E in Eq. (5) changes by a small amount, the value of τ changes considerably because E is in the exponent.

Equation (6) can be used with E_c and the moment of inertia for a methyl group $I=5.39\times10^{-47}$ kg m^2 to recast the fitted value $\tau_{c\infty}$ into the form $\tau_{c\infty}/\tilde{\tau}_{c\infty}=3.2$ for the two out-of-plane methyl groups in the *t*-butyl group. Given the crudeness of the simplistic classical harmonic oscillator model, this is a reasonable value for $\tau_{c\infty}/\tilde{\tau}_{c\infty}$. If the fitted value were several orders of magnitude greater than or less than unity, this would be cause for concern. It is not clear how applicable Eq. (6) is for $\tilde{\tau}_{b\infty}$ since τ_b characterizes the reorientation of both the (nearly) in-plane methyl group and the *t*-butyl group as a whole, presumably in some geared motion. If the moment of inertia for a methyl group is used in Eq. (6) then $\tau_{b\infty}/\tilde{\tau}_{b\infty,\mathrm{methyl}}=0.18$ and if the moment of inertia of a *t*-butyl group (approximated as 15 times that of a methyl group) is used, $\tau_{b\infty}/\tilde{\tau}_{b\infty,t-\mathrm{butyl}}=0.046$.

V. DISCUSSION

This paper is part of a long-range study, using low-frequency proton NMR relaxometry and x-ray diffraction, to investigate intramolecular reorientation in van der Waals solids made up of alkyl-substituted aromatic hydrocarbon molecules. We begin this discussion by considering some ethyl- and isopropyl-substituted aromatic molecular solids as a well-understood foundation. We then compare four closely related *t*-butyl systems in an attempt to set the stage for the formulation of a more general model, in future studies, for the reorientation of a *t*-butyl group and its constituent methyl groups in this class of molecular solids.

Relaxation rate data show unambiguously that in the solid state, ethyl groups[34,35] and isopropyl groups[34,36] attached to planar aromatic molecules are always static (on the NMR time scale) with respect to rotation of the alkyl group around the bond linking it to the aromatic ring system. Intermolecular interactions in the solid state prohibit these alkyl group rotations on the NMR time scale because the ethyl and isopropyl groups lack threefold symmetry. In these solids, only the terminal methyl groups of the ethyl and isopropyl groups reorient on the NMR time scale. This is in marked contrast to the gas phase, where ethyl and isopropyl groups attached to aromatic rings have rotation barriers that are *lower* than their constituent methyl group rotation barriers.[37–39] The barriers for rotation of the methyl groups in these solids are in the range 9–14 kJ mol^{-1}. These are ''textbook'' compounds with regard to the interpretation of the proton spin–lattice relaxation rate in terms of a model for methyl group reorientation. In this case one has a much simpler version of Eq. (2) [with Eqs. (3) and (4)] giving $R=A[2\tau/(1+\omega^2\tau^2)+8\tau/(1+4\omega^2\tau^2)]$ (or Z such terms if there are Z crystallographically inequivalent sites) with Eqs. (5) and (6) used to model τ. Indeed, it is found that $A/\tilde{A}=1$ and that $\tau_\infty/\tilde{\tau}_\infty$ is of order unity for these systems. These two observations, along with the observed ranges in barriers indicate (1) that it is indeed methyl groups that are reorienting on the NMR time scale, (2) that the appropriate proton spin–proton spin interactions are included in the model, and (3) that the simplest case of random hops described by Poisson statistics is all that is needed. This gives one confidence in the basic model. *We view the dynamical model used in these cases as essentially complete*, although there is much to be learned from understanding the 9–14 kJ mol^{-1} barrier range in terms of the different intramolecular and intermolecular contributions to the barrier for methyl group reorientation in these ethyl and isopropyl compounds in the solid state.

As a segue from the ethyl and isopropyl systems to the more complex *t*-butyl systems, we note, for comparison, that in the gas phase the methyl rotation barrier in ethane has been found by several different experimental methods to be about 12 kJ mol^{-1}; a recent determination by Fourier transform far-infrared torsional spectroscopy gives a value of 12.11 ± 0.01 kJ mol^{-1}.[40] It is now well understood theoretically that this barrier arises from the additional electronic stabilization of the staggered conformation relative to the eclipsed conformation of the methyl group.[41] Gas-phase methyl rotation barriers are not as well known for ethane derivatives that have additional alkyl substituents on the carbon atom to which the rotating methyl is bonded, but it appears that each such substituent may result in the barrier being raised by about 2–3 kJ mol^{-1}.[42]

In the solid state, the compounds with *t*-butyl substituents are more complex and more interesting than the compounds with ethyl and isopropyl substituents. We are aware of only four aromatic systems with *t*-butyl substituents for which *both* x-ray diffraction data *and* solid-state low-frequency NMR data are available: 4-methyl-2,6-di-*t*-butylphenol (**1**) (x-ray diffraction[43] and NMR relaxometry;[3,6,7] 3-*t*-butylchrysene (**2**) (as reported here); 1,4-di-*t*-butylbenzene (**3**) (x-ray diffraction[44] and NMR relaxometry[4]); and polymorph *A* of 2,6-di-*t*-butylnaphthalene (**4**) (x-ray diffraction[1,45] and NMR relaxometry[1,45]).[46] We compare here the relationship between the *t*-butyl group environment and the NMR relaxometry results for these four systems.

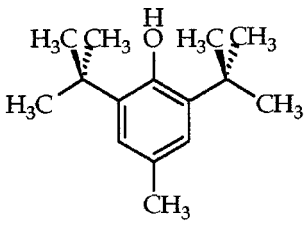

(**1**) 4-methyl-2,6-di-*t*-butylphenol

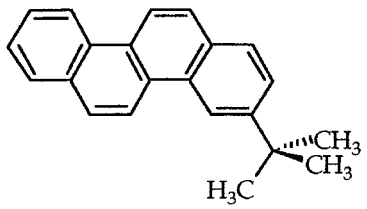

(**2**) 3-*t*-butylchrysene

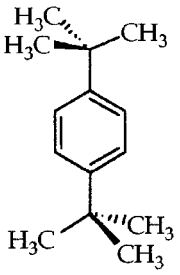

(**3**) 1,4-di-*t*-butylbenzene

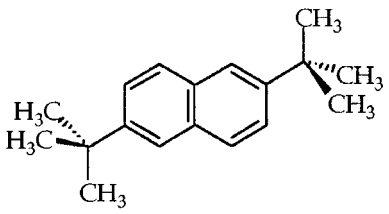

(**4**) 2,6-di-*t*-butylnaphthalene

The *t*-butyl groups of **1**–**4** in the solid state are found by x-ray crystallography to be oriented as indicated in the above-given drawings, with one methyl group lying with its carbon atom in the plane of the aromatic ring (or nearly so) and the other two methyl groups lying with their carbon atoms above and below that plane.

The energy barriers E_b and E_c, obtained from our relaxometry measurements for the four solids **1**–**4**, are listed in Table I. The value of E_b, the barrier for the synchronized reorientation of the *t*-butyl group and its in-plane (or nearly so) methyl group, decreases along the sequence **1**→**2**→**3**→**4**, while the value of E_c, the barrier for the reorientation of the two out-of-plane methyl groups, increases along this same sequence of the four solids. Further experimental and computational work will be needed before we can draw any conclusions about the significance of this intriguing reversal in the trends for E_b and E_c because the values of E_c for **2**, **3**, and **4** are very similar. At this time we can offer only a few qualitative interpretations for some of the trends observed in the barriers given in Table I.

For **1**, for example, we suggest that there are two important contributions to E_b: *inter*molecular steric interactions between the reorienting *t*-butyl group and neighboring molecules in the crystal, and *intra*molecular steric interactions between the *t*-butyl group and the OH substituent on the adjacent ring carbon (Fig. 5). In the low-energy conformation for **1** the OH group is situated in the gap between the two out-of-plane methyl groups of the *t*-butyl group, whereas in the transition structure for *t*-butyl rotation one of these methyl groups is severely crowded against the OH group (Fig. 5). This type of intramolecular steric effect is absent in **2**, **3**, and **4**, since the *t*-butyl groups in those three compounds are flanked on the aromatic rings only by hydrogen substituents, which are sterically much less demanding than the larger OH substituent in **1**. This can account for the observation that **1** has the largest value of E_b in Table I.

For the reorientation of the out-of-plane methyl groups in **1**, we suggest that the barrier E_c is dominated by intra-*t*-butyl electronic interactions analogous to those in ethane.[41] This defines the low-energy conformation and the transition structure as having staggered and eclipsed conformations, respectively, as illustrated in Fig. 6. In addition, however, we note that in a perfectly staggered low-energy conformation each out-of-plane methyl group would have one hydrogen that would lie about 2.3 Å from the hydroxyl oxygen, which is about 0.3 Å less than the sum of the van der Waals radii for hydrogen (1.2 Å) and oxygen (1.4 Å). In contrast, in a perfectly eclipsed transition structure the closest separation between a methyl hydrogen and the hydroxyl oxygen would be about 2.7 Å. This would result in a greater energy-raising steric effect in the low-energy conformation than in the tran-

TABLE I. Experimental values for reorientational barriers.[a]

	Compound	E_b (kJ mol^{-1})	E_c (kJ mol^{-1})	Refs.
1	4-methyl-2,6-di-*t*-butylphenol	34	10	6,7
2	3-*t*-butylchrysene	24	14	···
3	1,4-di-*t*-butylbenzene	19	16	4
4	2,6-di-*t*-butylnaphthalene	18	18	1,45

[a]All uncertainties are approximately ±1 kJ mol^{-1}.

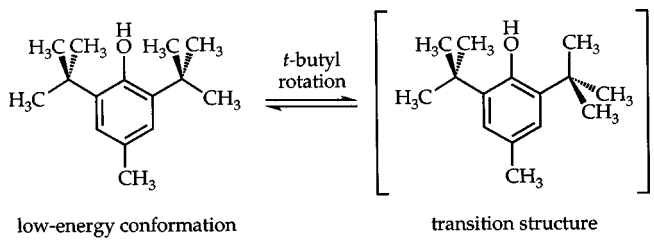

FIG. 5. Low-energy and transition structure conformations for *t*-butyl reorientation in 4-methyl-2,6-di-*t*-butylphenol (**1**).

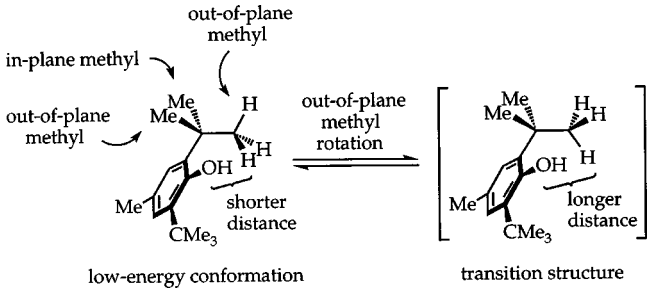

FIG. 6. Low-energy and transition structure conformations for out-of-plane methyl reorientation in 4-methyl-2,6-di-*t*-butylphenol (**1**).

sition structure, thereby decreasing the total barrier E_c. This type of barrier-lowering intramolecular steric effect is absent in **2**, **3**, and **4**, in which there are only small hydrogen substituents flanking the *t*-butyl group, which is in accord with the observation that **1** has the smallest value of E_c in Table I. Consistent with this proposed intramolecular steric interaction, E_c for **1** is 2 kJ mol^{-1} *lower* than the barrier for methyl reorientation in ethane.[40]

Turning now to **2**, **3**, and **4**, we suggest that intermolecular steric interactions are the main contributors to the E_b barriers, while intra-*t*-butyl electronic interactions are the main contributors to the E_c barriers. The E_b and E_c barriers for these three compounds each span only a rather narrow range (6 ± 2 kJ mol^{-1} for E_b, and 4 ± 2 kJ mol^{-1} for E_c). We suggest that the small *differences* among the E_b and also the E_c barriers for these three compounds arise mainly from slightly different amounts of intermolecular steric interactions in the low-energy conformations as compared with the transition structures for the reorientation of both the *t*-butyl and the out-of-plane methyl groups. The x-ray data show that there are no unusually close intermolecular atom-atom contacts in **2** (Figs. 2 and 3), that the *t*-butyl groups in **3** are nestled against the aromatic rings of neighboring molecules,[44] and that the *t*-butyl groups in **4** interact with the *t*-butyl groups on neighboring molecules.[1,45]

The qualitative explanations proposed here need to be quantified in the future, both by correlating the crystal structures with the observed barriers, and by computational studies. This work is in progress.

Prior to the present study, we had thought that there were only two extreme cases of *t*-butyl aromatic systems: those like **1** with two very distinct E_b and E_c barriers, and those like **4** with only one barrier. The current study, however, shows that the barriers for **2** are intermediate between those for **1** and those for **4**. Furthermore, although the data for **3** were fitted initially in the same manner employed for **4**, giving a single barrier, a later and more careful analysis revealed two distinct barriers[4] as listed in Table I. The results reported here for **2** and the reinterpreted data[4] for **3** strongly suggest a continuum of barriers.

VI. SUMMARY

We have synthesized 3-*t*-butylchrysene and correlated x-ray diffraction data in a single crystal and low-frequency NMR relaxometry data in a polycrystalline sample. The single-crystal x-ray data show that the four molecules in the unit cell are crystallographically identical, requiring a unique environment for *t*-butyl groups. One methyl group lies nearly in the plane of the adjacent ring and the other two methyl groups lie above and below this plane, respectively. There are no unusually close intermolecular atom–atom contacts.

The observed proton spin–lattice relaxation rate R has been modeled in terms of the reorientation for *t*-butyl groups and their constituent methyl groups. These motions modulate the proton spin–proton spin dipole–dipole interactions. We have used the simplest possible dynamical model, that of random rotors with a distribution of times between hops given by a Poisson distribution. We have shown the importance of both performing a relaxation rate study at more than one frequency *and* employing *low* NMR frequencies.

We have put this study into a larger context by comparing the results for 3-*t*-butylchrysene with three other *t*-butyl-substituted aromatic compounds. For these four compounds there appears to be a continuum of cases between the two extremes. At one extreme (4-methyl-2,6-di-*t*-butylphenol, **1**), the two out-of-plane methyl groups (above and below the plane of the aromatic ring) reorient with a barrier *lower* than that expected solely on the basis of intra-*t*-butyl electronic interactions, presumably because steric interactions with the neighboring OH group selectively *raise* the energy of the low-energy conformation. The *t*-butyl group in **1** (and its constituent in-plane methyl group) reorient synchronously, and much more slowly, with a barrier determined in part by the *difference* in intramolecular steric interactions of the *t*-butyl group with the flanking OH substituent on one of the adjacent ring carbons and the flanking hydrogen substituent on the other adjacent ring carbon. At the other extreme (polymorph *A* of 2,6-di-*t*-butylnaphthalene, **4**), the out-of-plane methyl groups have a *higher* barrier than in **1**, which we suggest can be attributed to two effects: the absence of *intra*molecular barrier-lowering steric effects (since both adjacent ring carbons bear hydrogen substituents), and the presence of *inter*molecular effects. In **4**, the *t*-butyl group and *all three* of its constituent methyl groups reorient synchronously; that is, they all have the same barrier within experimental uncertainty. In going from one of these extremes to the other among the set of four compounds, a pattern emerges: as the barrier for reorientation of the *t*-butyl group (and the in-plane methyl group) increases, the barrier for reorientation of the out-of-plane methyl groups decreases. We are proceeding with experimental and computational studies to develop a more precise understanding of the dependence of the E_b and E_c barriers on the intramolecular and intermolecular structures in crystals of *t*-butyl-substituted aromatic compounds.

[1] P. A. Beckmann, K. S. Burbank, K. Martin-Clemo *et al.*, J. Chem. Phys. **113**, 1958 (2000).
[2] G. H. Penner, J. M. Polson, C. Stuart, G. Ferguson, and B. Kaitner, J. Phys. Chem. **96**, 1521 (1992).
[3] J. M. Polson, J. D. D. Fyfe, and K. R. Jeffrey, J. Chem. Phys. **94**, 3381 (1991).
[4] P. A. Beckmann, Phys. Rev. B **39**, 12248 (1989).
[5] P. A. Beckmann, A. I. Hill, E. B. Kohler, and H. Yu, Phys. Rev. B **38**, 11098 (1988).

[6] P. A. Beckmann, F. A. Fusco, and A. E. O'Neill, J. Magn. Reson. **59**, 63 (1984).
[7] P. A. Beckmann, C. I. Ratcliffe, and B. A. Dunell, J. Magn. Reson. **32**, 391 (1978).
[8] M. B. Dunn and C. A. McDowell, Mol. Phys. **24**, 969 (1972).
[9] G. H. Stout and L. H. Jensen, *X-Ray Structure Determination: A Practical Guide* (Wiley, New York, 1989).
[10] M. Hashimoto, S. Hashimoto, H. Terao, M. Kuma, H. Niki, and H. Ino, Z. Naturforsch., A: Phys. Sci. **55a**, 167 (2000).
[11] H. Terao, M. Hashimoto, S. Hashimoto, and Y. Furukawa, Z. Naturforsch., A: Phys. Sci. **55a**, 230 (2000).
[12] J. Tritt-Goc, N. Pislewski, A. Pawlowski, and R. Goc, Solid State Commun. **106**, 367 (1998).
[13] J. Hatori, M. Komukae, T. Osaka, and Y. Makita, J. Phys. Soc. Jpn. **65**, 1960 (1996).
[14] R. Watanabe, T. Asaji, Y. Furukawa, and D. Nakamura, Z. Naturforsch., A: Phys. Sci. **44**, 1111 (1989).
[15] F. Imashiro, A. Saika, and Z. Taira, J. Org. Chem. **52**, 5727 (1987).
[16] K. Takegoshi, F. Imashiro, T. Tereo, and A. Saika, J. Chem. Phys. **80**, 1089 (1984).
[17] J. Virlet, L. Quiroga, B. Boucher, J. P. Amoureux, and M. Castelain, Mol. Phys. **48**, 1289 (1983), and references therein.
[18] B. Szafranska, H. Maluszynska, and Z. Pajak, Z. Naturforsch., A: Phys. Sci. **55**, 706 (2000).
[19] G. L. Hoatson, and R. L. Vold, in *NMR Basic Principles and Progress*, edited by P. Diehl, E. Fluck, H. Günther, R. Kosfeld, and J. Seelig (Springer, Berlin, 1994), Vol. 32, p. 1.
[20] A. J. Vega and Z. Luz, J. Chem. Phys. **86**, 1803 (1987).
[21] C. P. Slichter, *Principles of Magnetic Resonance*, 3rd ed. (Springer, Berlin, 1990).
[22] A. Abragam, *The Principles of Nuclear Magnetism* (Oxford University Press, Oxford, 1961).
[23] D. van der Putten, G. Diezemann, F. Fujara, K. Hartmann, and H. Sillescu, J. Chem. Phys. **96**, 1748 (1992).
[24] M. Anderson, L. Bosio, J. Bruneaux-Poulle, and R. Fourme, J. Chim. Phys. Phys.-Chim. Biol. **74**, 68 (1977).
[25] P. Speier, H. Zimmerman, U. Haeberlen, and Z. Luz, Mol. Phys. **95**, 1153 (1998).
[26] N. Karl, H. Heym, and J. J. Stezowski, Mol. Cryst. Liq. Cryst. **131**, 163 (1985).
[27] G. H. Penner, Y.-C. P. Chang, P. Nechala, and R. Froese, J. Org. Chem. **64**, 447 (1999).
[28] F. B. Mallory and C. W. Mallory, Organic Reactions **30**, 1 (1984).
[29] Elemental analyses by M-H-W Laboratories, P.O. Box 15149, Phoenix, AZ 85018.
[30] Assignments confirmed by COSY experiments.
[31] C. Palmer, A. M. Albano, and P. A. Beckmann, Physica B **190**, 267 (1993).
[32] N. L. Owen, in *Internal Rotation in Molecules*, edited by W. J. Orville-Thomas (Wiley, New York, 1974), p. 157.
[33] C. Palmer, Ph.D. thesis, Bryn Mawr College, 1991.
[34] P. A. Beckmann, C. A. Buser, C. W. Mallory, F. B. Mallory, and J. Mosher, Solid State Nucl. Magn. Reson. **12**, 251 (1998).
[35] P. A. Beckmann, L. Happersett, A. V. Herzog, and W. M. Tong, J. Chem. Phys. **95**, 828 (1991).
[36] H. A. Al-Hallaq and P. A. Beckmann, J. Chem. Soc., Faraday Trans. **89**, 3801 (1993).
[37] A. Miller and D. W. Scott, J. Chem. Phys. **68**, 1317 (1978).
[38] T. Schaefer, W. J. E. Parr, and W. Danchura, J. Magn. Reson. **25**, 167 (1977).
[39] T. Schaefer, L. Kruczynski, and W. Niemczura, Chem. Phys. Lett. **38**, 498 (1976).
[40] N. Moazzen-Ahmadi, H. P. Gush, M. Halpern, H. Jagannath, A. Leung, and I. Ozier, J. Chem. Phys. **88**, 563 (1988).
[41] V. Pophristic and L. Goodman, Nature (London) **411**, 565 (2001).
[42] S. Weiss and G. E. Leroi, Spectrochim. Acta, Part A **25A**, 1759 (1969).
[43] M. Bolte and M. Amon (private communication). The data for this structure may be obtained free of charge by contacting the Cambridge Crystallographic Data Centre at deposit@ccdc.cam.ac.uk. Reference code MBPHOL02.
[44] M. A. Kravers, M. Yu Antipin, and Yu T. Struchkov, Cryst. Struct. Commun. **9**, 955, (1980).
[45] A. L. Rheingold, J. S. Figueroa, C. Dybowski, and P. A. Beckmann, Chem. Commun. (Cambridge) **2000**, 651.
[46] A second polymorph of 2,6-di-*t*-butylnaphtalene also has been studied (Ref. 45).